EUROPEAN SOCIETY OF RADIOLOGY
Insights into Imaging

ORIGINAL ARTICLE   **Open Access**

Accelerated 3D whole-heart non-contrast-enhanced mDIXON coronary MR angiography using deep learning-constrained compressed sensing reconstruction

Xi Wu[1], Xun Yue[2], Pengfei Peng[2], Xianzheng Tan[1], Feng Huang[1], Lei Cai[2], Lei Li[2], Shuai He[2], Xiaoyong Zhang[3], Peng Liu[1] and Jiayu Sun[2]*

Abstract

Objectives To investigate the feasibility of a deep learning-constrained compressed sensing (DL-CS) method in non-contrast-enhanced modified DIXON (mDIXON) coronary magnetic resonance angiography (MRA) and compare its diagnostic accuracy using coronary CT angiography (CCTA) as a reference standard.

Methods Ninety-nine participants were prospectively recruited for this study. Thirty healthy subjects (age range: 20–65 years; 50% female) underwent three non-contrast mDIXON-based coronary MRA sequences including DL-CS, CS, and conventional sequences. The three groups were compared based on the scan time, subjective image quality score, signal-to-noise ratio (SNR), and contrast-to-noise ratio (CNR). The remaining 69 patients suspected of coronary artery disease (CAD) (age range: 39–83 years; 51% female) underwent the DL-CS coronary MRA and its diagnostic performance was compared with that of CCTA.

Results The scan time for the DL-CS and CS sequences was notably shorter than that of the conventional sequence (9.6 ± 3.1 min vs 10.0 ± 3.4 min vs 13.0 ± 4.9 min; $p < 0.001$). The DL-CS sequence obtained the highest image quality score, mean SNR, and CNR compared to CS and conventional methods (all $p < 0.001$). Compared to CCTA, the accuracy, sensitivity, and specificity of DL-CS mDIXON coronary MRA per patient were 84.1%, 92.0%, and 79.5%; those per vessel were 90.3%, 82.6%, and 92.5%; and those per segment were 98.0%, 85.1%, and 98.0%, respectively.

Conclusion The DL-CS mDIXON coronary MRA provided superior image quality and short scan time for visualizing coronary arteries in healthy individuals and demonstrated high diagnostic value compared to CCTA in CAD patients.

Critical relevance statement DL-CS resulted in improved image quality with an acceptable scan time, and demonstrated excellent diagnostic performance compared to CCTA, which could be an alternative to enhance the workflow of coronary MRA.

Key Points

- Current coronary MRA techniques are limited by scan time and the need for noise reduction.
- DL-CS reduced the scan time in coronary MR angiography.
- Deep learning achieved the highest image quality among the three methods.
- Deep learning-based coronary MR angiography demonstrated high performance compared to CT angiography.

---

*Correspondence:
Jiayu Sun
cardiac_wchscu@163.com
Full list of author information is available at the end of the article

Springer Open

Wu *et al. Insights into Imaging* (2024)15:224

Page 2 of 12

Graphical Abstract

Accelerated 3D whole-heart non-contrast-enhanced mDIXON coronary MR angiography using deep learning-constrained compressed sensing reconstruction

Deep learning-constrained compressed sensing resulted in notably improved image quality with a clinically acceptable scan time and demonstrated excellent diagnostic performance when compared to coronary CTA as the reference standard, which could be a viable alternative to enhance the clinical workflow of coronary MRA.
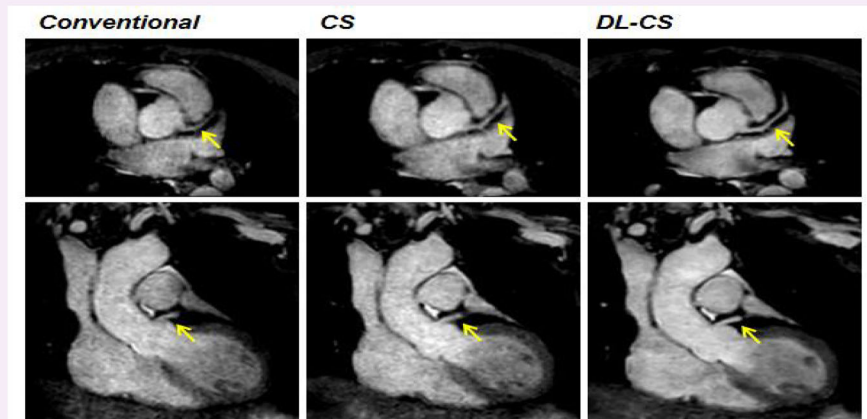
Insights Imaging (2024) Wu X, Yue X, Peng PF et al.
DOI: 10.1186/s13244-024-01797-3

Introduction

Whole-heart coronary magnetic resonance angiography (MRA) is a noninvasive and radiation-free imaging technique that holds promise for the assessment of coronary arteries [1–3]. MRA has demonstrated high sensitivity, specificity, and negative predictive value for diagnosing coronary artery diseases (CAD) across various clinical scenarios [4]. Currently, the 3D balanced steady-state free precession (bSSFP) sequence is preferred to others for coronary artery visualization [1, 5–8]. However, this imaging technique is sensitive to flow and susceptible to artifacts, which eventually affect image quality [9]. Recent studies performed water–fat separation DIXON-based methods for coronary MRA, revealing substantial enhancement in image quality due to its low susceptibility to field inhomogeneity [10–12]. Additionally, this approach also provides additional available fat information and assists in identifying vascular calcification, luminal stenosis, and plaque burden [13–15]. Furthermore, the modified DIXON (mDIXON) approach provides images with excellent quality and enhanced vessel-lumen-to-fat contrast, and allows an additional signal-to-noise ratio (SNR) boost [9, 16, 17].

Currently, the use of whole-heart mDIXON-based strategies in assessing coronary arteries faces limitations due to the inherent small caliber of coronary arteries, which impedes its routine application in clinical practice [12, 18, 19]. Firstly, the extended scan time may lead to heart rate and respiratory pattern drift, bulk motion, and consequent degradation of the final image quality [12]. Secondly, while higher spatial resolution is highly desirable for coronary MRA, it compromises SNR which is directly proportional to the voxel size [20]. Thus, effective noise removal is essential for high-resolution coronary MRA. There remains an unmet need to reduce the scan time of 3D high-resolution coronary MRA sequences in clinical practice.

Novel approaches such as parallel accelerated techniques and compressed sensing (CS)-based methods enable rapid data acquisition. The use of parallel accelerated techniques, such as sensitivity encoding (SENSE), has led to reduced image acquisition times while maintaining image quality in coronary MRA [21–24]. Despite its promising result, limitations are raised with specific artifacts, including residual aliasing and g-factor noise enhancement, due to the high acceleration factor

Wu *et al. Insights into Imaging* (2024)15:224

Page 3 of 12

associated with parallel accelerated techniques [25]. CS-based techniques, which involve fast acquisition through random undersampling of *k*-space combined with iterative image reconstruction, have shown potential in producing higher overall image quality compared to conventional parallel accelerated techniques in coronary MRA [12, 18, 26]. Despite these advancements, selecting optimal sparsity transforms and addressing artifacts remain significant challenges in CS-based techniques, especially with very high acceleration factors leading to the potential reduction in image quality due to insufficient noise removal during reconstruction [27].

Recently, the integration of deep learning (DL) into MR acquisition has demonstrated promising results in enhancing image quality or speeding up the process in coronary MRA [20, 28–32]. However, such a technique, involves training a neural network to identify the most effective transformation from the zero-filled *k*-space to the desired reconstruction. A novel convolutional neural network incorporates multiscale sparsification in a learnable manner to substitute traditional sparsifying transforms and improve the CS approach [33]. The DL-constrained compressed sensing (DL-CS) method, employing the Adaptive-CSNetwork scheme, has shown superior performance in MR reconstructions [28, 34–36]. A useful strategy for achieving a rapid 3D mDIXON coronary MRA would exploit the advantage of CS theory and DL algorithms.

This study aimed to investigate the feasibility of using DL algorithms to enhance image quality in the CS-based non-contrast-enhanced mDIXON coronary MRA. We intended to fully evaluate its performance in both healthy subjects and patients suspected of CAD and hypothesized that the DL-CS technique would expand the scope of clinical application of mDIXON coronary MRA with improved image quality.

Materials and methods
Study participants
Ninety-nine participants were prospectively enrolled in this study between October 2021 and January 2023. The study included two subgroups: 30 healthy volunteers (15 females; age range, 20–65 years) with no medical conditions that could interfere with the acquisition and analysis, and 69 patients (35 females; age range, 39–83 years) suspected of CAD scheduled for coronary computed tomography angiography (CCTA). Subjects with pacemakers, defibrillators, or other general contraindications were excluded from the study. No beta-blocker or nitroglycerin was administered to any of the subjects. The institutional review board approved this prospective study, and all study population provided written informed consent.

MRA protocol
A 3-T MR scanner (Ingenia Elition, Philips Healthcare) equipped with a 16-channel body matrix coil and a 12-channel spine matrix coil was used to perform the coronary MRA examinations. Electrocardiography-triggered and respiratory navigator-gated techniques were used during the entire process of the scan. To identify the relatively quiescent time of the right coronary artery (RCA), one hundred cardiac phase four-chamber images were obtained during the free-breathing of the participants, allowing for the determination of the optimal acquisition window and delay time for the scan. For coronary artery imaging, all healthy volunteers underwent three non-contrast mDIXON coronary MRA scans, including DL-CS, CS, and conventional SENSE approaches. The scan order of the three sequences was randomized for each subject. For patients with suspected CAD, coronary MRA was obtained using the DL-CS sequence. The scanning parameters are presented in Table 1.

CCTA protocol
All patients also received CCTA utilizing a 256-row CT scanner with a 16 cm wide detector (Revolution CT, GE Healthcare). All examinations were obtained using the prospective ECG-triggered axial acquisition scan mode. Specific scan parameters included a gantry rotation time of 0.28 s, an automatically adjusted tube current range between 400 mA and 800 mA, a tube voltage of 120 kV, and a slice thickness of 0.625 mm using the "stand" reconstruction kernel. Iodinated contrast material (Iomeprol Injection, concentration 400 mgI/mL) was administered to each patient at a traditional weight-dependent rate of 32 mgI/kg/s for a 10-s injection time. The injection flow rate was set by dividing the total contrast volume by the 10-s injection time. Following contrast injection, 30 mL of saline was administered at the same flow rate.

Image analysis
Each acquisition time was recorded for each volunteer. All original MR images were transferred to the post-processing workstation (IntelliSpace Portal version 9.0.5; Philips Healthcare) for quality assessment.

Healthy subject study
Qualitative image analysis
Four radiologists independently evaluated all the coronary MRA images and blindly to the scan protocol. The quality of coronary artery visualization was assessed using a five-point scale: five for excellent, coronary vessels with clear edges, minimal image noise and no apparent artifacts; four for good, coronary vessels with clear edges, mild image noise and artifacts; three for average, coronary vessels with adequate edges, moderate image noise and artifacts; two for poor, coronary vessels with blurred

Wu *et al. Insights into Imaging* (2024)15:224

Page 4 of 12

Table 1 Image parameters

	DL-CS	CS	Conventional
Sequence type	Spoiled gradient echo	Spoiled gradient echo	Spoiled gradient echo
Fat suppression	mDIXON	mDIXON	mDIXON
TR/TE1/TE2 (ms)	4.10/1.32/2.40	4.10/1.32/2.40	4.10/1.32/2.40
Field of view (mm^3)	$265 \times 301 \times 112$	$265 \times 301 \times 112$	$265 \times 301 \times 112$
Matrix	$176 \times 201 \times 150$	$176 \times 201 \times 150$	$176 \times 201 \times 150$
Acceleration factor	CS 5	CS 5	SENSE 4
Acquisition voxel size (mm^3)	$1.50 \times 1.50 \times 1.50$	$1.50 \times 1.50 \times 1.50$	$1.50 \times 1.50 \times 1.50$
Reconstruction voxel size (mm^3)	$0.75 \times 0.75 \times 0.75$	$0.75 \times 0.75 \times 0.75$	$0.75 \times 0.75 \times 0.75$
Bandwidth (Hz/pixel units)	0.36	0.36	0.36
Scale factor	0.6	0.6	0.6
T2 preparation duration (ms)	30	30	30
Acceptance window	5	5	5
Flip angle (degree)	10	10	10

CS compressed sensing, *DL* deep learning, *SENSE* sensitivity encoding

edges, high image noise, and severe artifacts; one for not visible. An image with a score of 3 or higher was deemed satisfactory and suitable for diagnosis. The original image quality scores from the four readers were utilized to assess consistency, while the final score for each participant was determined through negotiation among the four readers and was utilized for comparison between the three sequences.

Quantitative objective assessment

SNR and contrast-to-noise ratio (CNR) of the original image were calculated to compare the three techniques. For the measurement of blood intensity in the coronary arteries, the region of interest (ROI) was carefully placed in the lumen of the proximal areas of the LAD, left circumflex (LCX), and RCA, with the ROI size set as large as possible (2–5 mm) to mitigate partial volume effects. The myocardium adjacent to each coronary artery was selected to measure the myocardial signal intensity (SI). The noise was determined using the mean standard deviation (SD) of pixel values from two large air ROIs selected outside of the body. Similar ROIs were used in all image sets from the three sequences for each patient unless artery motion was detected. The following equations were used to calculate SNR and CNR [5]:

$$SNR = Mean(SI_{coronary\ artery})/SD_{air}$$

$$CNR = (SI_{coronary\ artery} - SI_{myocardium})/SD_{air}$$

Patient study

An observer evaluated the diagnostic performance of DL-CS mDIXON coronary MRA, who was blinded to participants' clinical information and the results of CCTA. The luminal diameter reduction of $\geq 50\%$ in a reference diameter ≥ 1.5 mm was defined as significant coronary vessel stenosis [37]. Two independent observers analyzed significant stenosis on CCTA images with CCTA serving as the non-invasive clinical reference standard. Consensus was reached through negotiation in case of disagreement. The number of stenoses on coronary MRA and its diagnostic performance for detecting significant stenosis, including sensitivity, specificity, positive predictive value (PPV), negative predictive value (NPV), and accuracy on a per-patient, per-vessel, and per-segment basis, were evaluated in comparison to CCTA.

Statistical analysis

Statistical analysis was conducted using the SPSS statistical software (version 25.0) and MedCalc software (version 19.3). All continuous variables were presented as mean ± SD. Friedman's test was employed to assess the mean scan time, visual evaluation scores, SNR, and CNR of the three sequences. The weighted Kappa test was utilized to evaluate the inter-observer agreement (kappa value > 0.7 was considered excellent, 0.4–0.7 was considered good, and < 0.4 was considered bad) [38]. Bland–Altman analysis was used to visually compare the difference between paired measures against their averages. A *p*-value of less than 0.05 indicated a statistical difference.

Results

The based characteristics for all participants are shown in Tables 2 and 3. All coronary MRA acquisitions were successfully performed for all healthy volunteers and patients suspected of CAD.

Wu *et al. Insights into Imaging* (2024)15:224

Page 5 of 12

Table 2 The characteristics of the healthy subjects ($n = 30$)

Characteristics	Results
Age (y)	28 ± 11
Age range (y)	20–65
Sex (female/male)	15/15
Height (cm)	166 ± 9
Weight (kg)	61 ± 14
Body mass index (kg/m^2)	21.7 ± 3.1
Systolic blood pressure (mmHg)	116 ± 14
Diastolic blood pressure (mmHg)	77 ± 10
Heart rate (beats/min)	74.0 ± 8.7

Healthy subject study

For healthy subjects, the acquisition time of the DL-CS and CS coronary MRA was shorter compared to the conventional method (9.6 ± 3.1 min vs 10.0 ± 3.4 min vs 13.0 ± 4.9 min; $p < 0.001$), with no significant difference between DL-CS and CS methods ($p > 0.05$).

Qualitative image analysis

Regarding the subjective evaluation of image quality, the DL-CS group achieved the highest quality scores than the conventional and CS coronary MRA (4.10 ± 0.96 vs 3.33 ± 0.99 vs 3.27 ± 1.01, $p < 0.001$). However, no significant difference in quality score was observed between the conventional and CS approaches ($p > 0.05$). The comparison of subjective image quality among the three sequences is shown in Supplementary Table 1. The weighted kappa value for inter-observer agreement for image quality score was excellent (kappa = 0.75–0.97).

Quantitative objective assessment

Among 30 healthy participants, 440 coronary segments with a diameter ≥ 1.5 mm were identified, with 438 (99.5%) for the DL-CS, 429 (97.5%) for the CS, and 426 (96.8%) for the conventional method available for evaluation. The SNRs and CNRs are summarized in Table 4. The SNRs and CNRs of DL-CS were highest among the three techniques ($p < 0.001$), but those were no significant differences in the conventional and CS coronary MRA approaches ($p > 0.05$). The comparison of image qualities among three groups in showing the origins and proximal courses of the left coronary artery is depicted in Fig. 1 and representative CPR images of three methods from two healthy volunteers are shown in Figs. 2 and 3, where the DL-CS showed superior image quality with fewer blurring artifacts. The Bland–Altman analysis indicated acceptable agreement for the DL-CS—conventional, CS—conventional, and DL-CS—CS pairs concerning their corresponding SNRs and CNRs (Fig. 4).

Table 3 Baseline characteristics for the patient study

Characteristics	Results
Age (years)	59 ± 10
Sex (female/male)	35/34
Body mass index (kg/m^2)	24.0 ± 3.1
Hemodynamic data	
Resting SBP (mmHg)	135 ± 20
Resting DBP (mmHg)	86 ± 9
Heart rate (beats/min)	74 ± 11
Cardiovascular risk factors	
Hypertension, *n* (%)	28 (40.6)
Hyperlipidemia, *n* (%)	28 (40.6)
Diabetes mellitus, *n* (%)	9 (13)
Prior myocardial infarction, *n* (%)	4 (5.8)
Smoking, *n* (%)	24 (34.8)
Family history of CAD, *n* (%)	12 (17.4)
Significant disease prevalence of CAD, *n* (%)	25 (36.2)
1 Coronary vessel disease, *n* (%)	13 (18.8)
2 Coronary vessel disease, *n* (%)	4 (5.8)
3 Coronary vessel disease, *n* (%)	8 (11.6)
CAC score prevalence	
0, *n* (%)	26 (37.7)
1–100, *n* (%)	15 (21.7)
101–300, *n* (%)	12 (17.4)
> 300, *n* (%)	16 (23.2)
CAD-RADS score	
0–2 (< 50% stenosis), *n* (%)	44 (63.8)
3 (50–69% stenosis), *n* (%)	12 (17.4)
4 (70–99% stenosis), *n* (%)	13 (18.8)

CAC coronary artery calcium, *CAD* coronary artery disease, *CAD-RADS* coronary artery disease-reporting and data system, *DBP* diastolic blood pressure, *SBP* systolic blood pressure

Table 4 Comparison of SNRs and CNRs from three methods with mDIXON coronary MRA

	Conventional	CS	DL-CS
Mean SNR	58.88 ± 16.98	59.24 ± 14.71	76.06 ± 15.93[a,b]
RCA	62.42 ± 20.38	61.73 ± 16.50	79.65 ± 18.77[a,b]
LAD	56.19 ± 14.89	57.48 ± 17.08	73.40 ± 17.07[a,b]
LCX	58.02 ± 20.92	58.51 ± 15.77	75.12 ± 17.88[a,b]
Mean CNR	17.61 ± 7.71	19.00 ± 7.87	29.70 ± 8.67[a,b]
RCA	21.10 ± 11.31	22.36 ± 10.34	34.61 ± 12.95[a,b]
LAD	15.85 ± 10.13	16.91 ± 10.90	26.02 ± 11.38[a,b]
LCX	15.88 ± 11.51	17.73 ± 9.68	28.48 ± 11.37[a,b]

CNR contrast-to-noise ratio, *CS* compressed sensing, *DL* deep learning, *LAD* left anterior descending artery, *LCX* left circumflex, *RCA* right coronary artery, *SNR* signal-to-noise ratio
[a] DL-CS vs conventional, $p < 0.001$
[b] DL-CS vs CS, $p < 0.001$

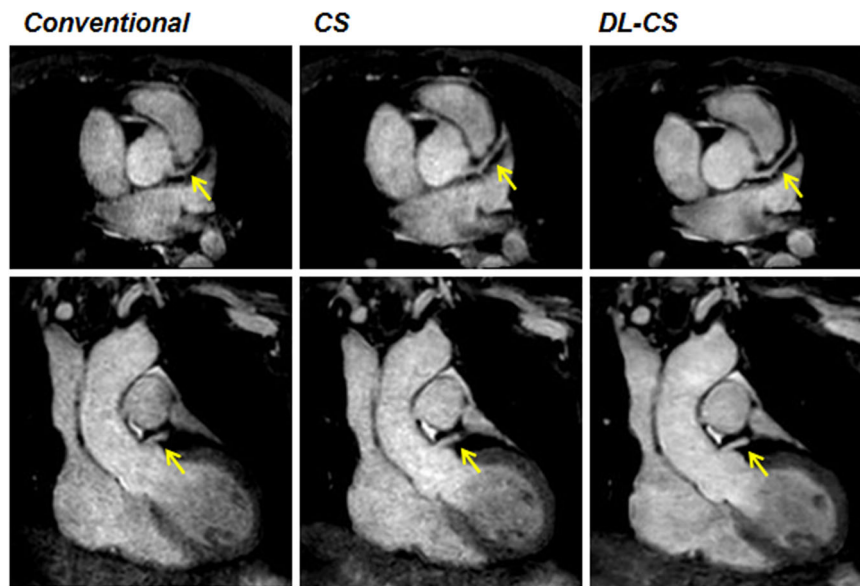Wu *et al. Insights into Imaging* (2024)15:224

Page 6 of 12

Fig. 1 A 49-year-old female volunteer. Comparison of image qualities among the three mDIXON sequences in visualizing the origins and proximal courses of the left coronary artery. CS, compressed sensing; DL, deep learning

Patient study

Twenty-five out of the sixty-nine patients presented with significant CAD on CCTA. Cardiovascular risk factors, and significant disease prevalence of CAD are shown in Table 3. The acquisition time interval between the coronary MRA and the CCTA ranged from 0 day to 15 days, with an average of 2 days.

Among the 69 patients, CCTA images revealed 930 segments with a reference luminal diameter ≥ 1.5 mm, out of which 885 segments (95.2%) in the coronary MRA were deemed diagnostic. The per-patient sensitivity, specificity, PPV, NPV, and accuracy of DL-CS coronary MRA were 92.0%, 79.5%, 71.9%, 94.6%, and 84.1%, respectively, those per vessel were 82.6%, 92.5%, 76.0%, 94.9%, and 90.3%, respectively, and those per segment were 85.1%, 98.0%, 79.7%, 98.6%, and 96.9%, respectively (Table 5). Representative coronary MRA and CCTA images of patients are depicted in Figs. 5 and 6.

Discussion

This study assessed a DL-CS approach with 3D wholeheart non-contrast-enhanced mDIXON coronary MRA in both healthy subjects and patients suspected of CAD. The preliminary results revealed that the DL-CS sequence could provide higher SNR and CNR, along with favorable image quality for visualizing coronary arteries in a short acquisition time compared to conventional and CS approaches in healthy subjects. Furthermore, it exhibited excellent diagnostic performance in patients, with CCTA serving as the reference standard.

DIXON-based strategies showed promising results in coronary MRA because of their unique advantages [10–12]. Given that coronary arteries are surrounded by epicardial fat, inadequate fat suppression can compromise vessel delineation [10]. Previous studies have indicated that the DIXON-based method, when compared to conventional fat suppression, improved coronary MRA image quality at both 1.5 T [39] and 3.0 T [10]. Additionally, compared to bSSFP, the DIXON-based technique displayed reduced sensitivity to magnetic field inhomogeneities [17, 40], resulting in fewer artifacts and enhanced vessel wall sharpness at distal anatomical borders [9]. Moreover, the presence of residual high-intensity fat signals can lead to motion-induced ghosting artifacts, negatively impacting image quality [41]. Leveraging the phase shifts caused by water–fat resonance frequency difference, the Dixon-based technique can separate water from fat, potentially reducing susceptibility to motion artifacts in the water images [10].

The DL-CS method demonstrated promising potential for rapid mDIXON coronary MRA. The major challenge in whole-heart coronary MRA has been the extended scan time, leading to motion artifacts. Parallel accelerated techniques [21–23] and CS-based accelerated methods [18, 26] could be used for fast data acquisition. Previous studies have shown that CS-based coronary MRA can reduce the scan time with favorable image quality compared to conventional parallel accelerated approaches [12, 18, 42]. Recently, DL reconstruction has been proposed for de-noising in coronary MRA [3]. Leveraging the
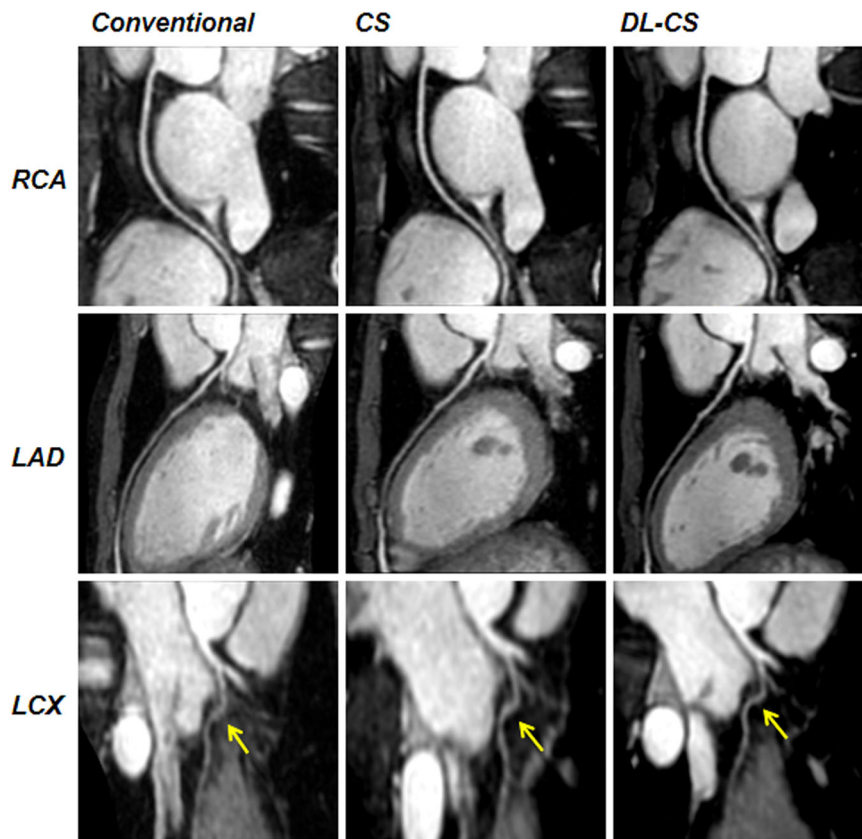
Fig. 2 The curved planar reformation images were obtained from a healthy 21-year-old male participant using conventional, CS, and DL-CS mDIXON coronary MRA sequences. The image quality of the RCA, LAD artery, and left circumflex on the DL-CS image was superior to the conventional and CS methods, especially on the LCX visualization (yellow arrows). CS, compressed sensing; DL, deep learning; LAD, left anterior descending artery; LCX, left circumflex; RCA, right coronary artery
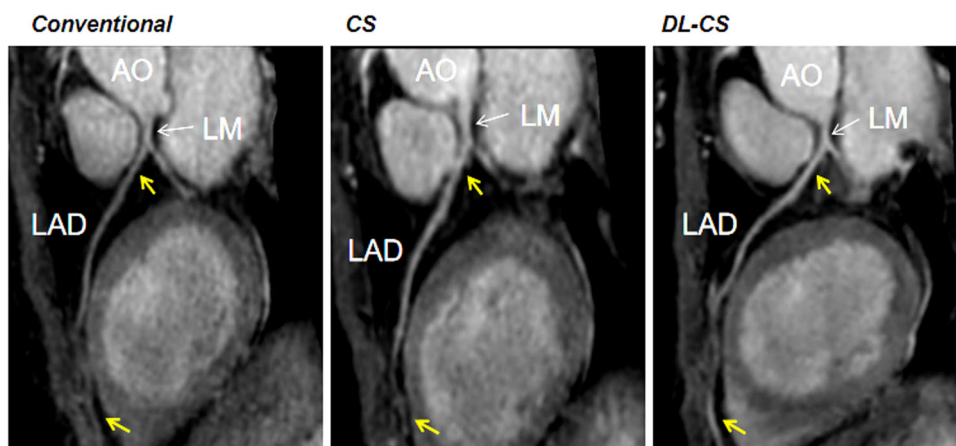

Fig. 3 Curved planar reformation images of the LAD from three coronary MRA approaches were obtained from a healthy 49-year-old female participant. The proximal and distal segments in the conventional and CS images exhibited less clarity compared to the DL-CS image (yellow arrows). AO, aorta; CS, compressed sensing; DL, deep learning; LAD, left anterior descending artery; LM, left main artery
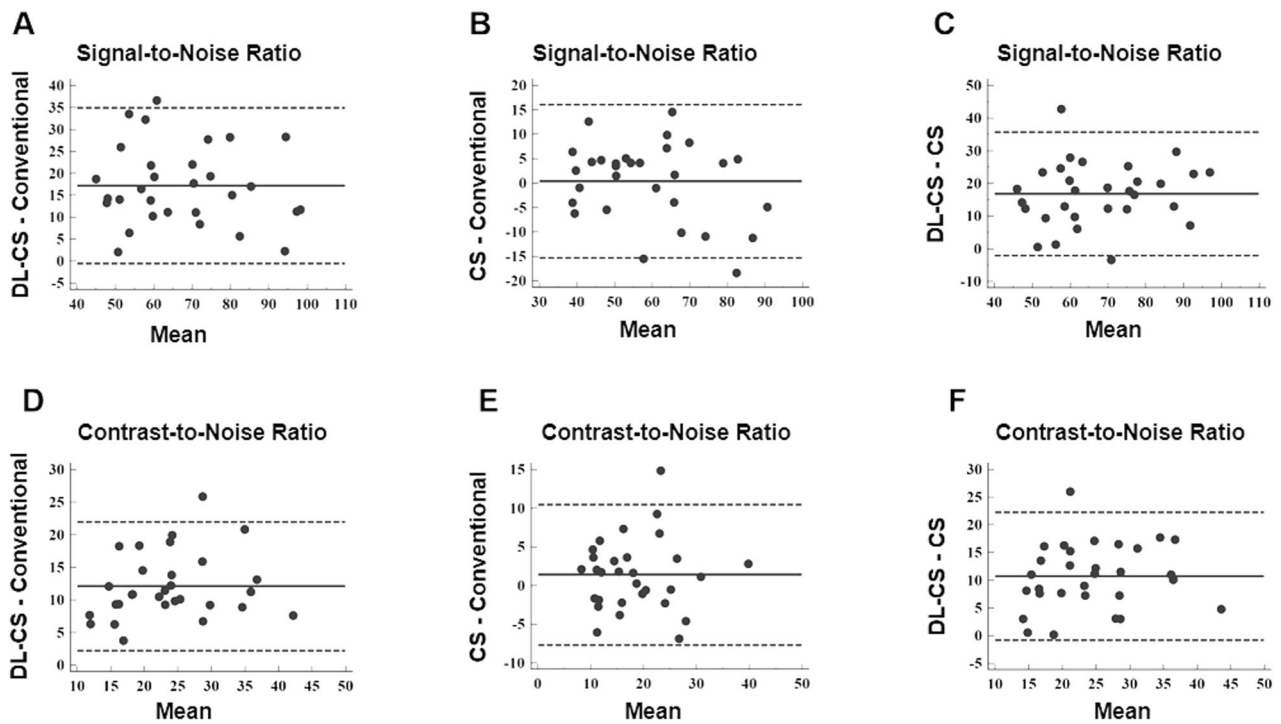
Wu *et al. Insights into Imaging* (2024)15:224

Page 8 of 12

Fig. 4 Bland–Altman analysis for SNR and CNR for DL-CS—conventional (**A**, **D**), CS—conventional (**B**, **E**), and DL-CS—CS (**C**, **F**). The y-axis provided the difference between the paired measures, while the x-axis provided the mean of the paired measures. The solid and dotted lines provided the mean difference and the 95% limits of agreement. CS, compressed sensing; DL, deep learning

Table 5 Diagnostic performance of DL-CS mDIXON coronary MRA in detecting significant CAD as defined by CCTA

	Accuracy (%)	Sensitivity (%)	Specificity (%)	PPV (%)	NPV (%)
Per patient	84.1 (58/69)	92.0 (23/25)	79.5 (35/44)	71.9 (23/32)	94.6 (35/37)
Per vessel	90.3 (187/207)	82.6 (38/46)	92.5 (149/161)	76.0 (38/50)	94.9 (149/157)
RCA	91.3 (63/69)	81.8 (9/11)	93.1 (54/58)	69.2 (9/13)	96.4 (54/56)
LAD	88.4 (61/69)	80.0 (20/25)	93.2 (41/44)	87.0 (20/23)	89.1 (41/46)
LCX	91.3 (63/69)	90.0 (9/10)	91.5 (54/59)	64.3 (9/14)	98.2 (54/55)
Per segment	96.9 (857/884)	85.1 (63/74)	98.0 (794/810)	79.7 (63/79)	98.6 (794/805)

LAD left anterior descending, *LCX* left circumflex, *NPV* negative predictive value, *PPV* positive predictive value, *RCA* right coronary artery

"learning noise" strategy, DL can effectively optimize the de-noising level and preserve a good edge, resulting in improved image quality [3]. High image quality was obtained using the DL-based reconstruction, which indicated that the DL method reduced image noise to preserve image quality while obtaining high spatial resolution [20, 43]. Yokota et al [20] evaluated the effects of DL reconstruction on image quality of high-resolution coronary MRA with ten healthy volunteers at 3 T. Additionally, Qi et al [29] and Fuin et al [30] developed DL techniques for bSSFP coronary MRA on a 1.5-T MR scanner. Hosseini et al [31] proposed the use of self-consistent robust artificial neural networks for k-space interpolation to enhance coronary MRA reconstruction quality. In contrast, our study combined CS and DL to achieve rapid 3D mDIXON coronary MRA, which exploited the advantage based on CS theory and DL algorithm. The DL-CS approach significantly reduced acquisition time compared to conventional methods, while also improving SNR, CNR, and image quality when
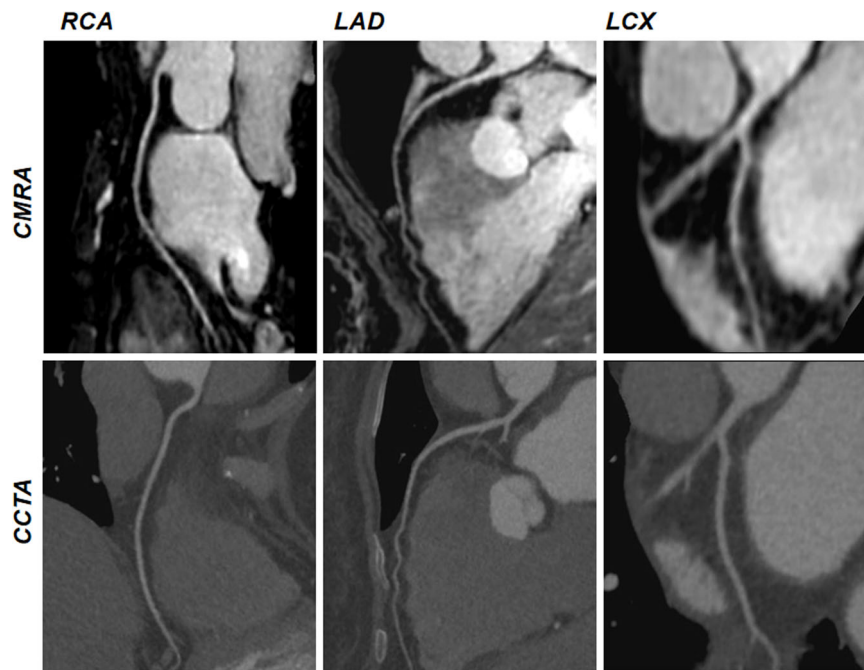
Wu *et al. Insights into Imaging* (2024)15:224

Page 9 of 12

Fig. 5 Non-contrast DL-CS mDIXON coronary MRA images of a 60-year-old female patient with normal coronary arteries. coronary MRA images are depicted in the top row, displaying the right coronary artery, LAD artery, and left circumflex. The corresponding reformatted images obtained with contrast-enhanced CCTA are shown in the bottom row. CMRA, coronary magnetic resonance angiography; CCTA, coronary computed tomography angiography

compared to CS and conventional methods in healthy subjects. Furthermore, DL-CS coronary MRA successfully demonstrated excellent diagnostic performance in 69 patients suspected of CAD, using CCTA as the reference standard. Especially, for patients with pregnancy or hypersensitivity to iodinated contrast agents, non-contrast-enhanced coronary MRA could be an alternative modality for CCTA.

Several additional critical aspects of the mDIXON coronary MRA were considered in this study. To mitigate bias, the DL-CS, CS, and conventional sequences were scanned in random order. As the scan time increases, so does the patient's fatigue and movement, as well as changes in respiration condition and heart rate, ultimately reducing acquisition efficiency and compromising image quality. Additionally, we employed one hundred cardiac phase images to identify a relatively quiescent period for imaging coronary arteries, recognizing the significant impact of heart rate on image quality. For patients with a high heart rate, the acquisition window was generally set at end-systole to obtain good image quality, consistent with findings by Wu et al [44]. Certainly, pre-scan breathing training and instructions to maintain calm breathing during the scan are also critical for obtaining high-quality coronary artery images.

Several limitations were present in this study. The image quality did not allow for a completely blinded evaluation, as DL-CS coronary images were easily distinguishable from conventional and CS coronary images due to reduced noise and superior image quality. For healthy participants, there was no reference standard (e.g., CCTA) available for comparing coronary artery image quality among the three groups. Furthermore, it is important to note that the patients included in this study did not undergo invasive coronary X-ray angiography as the "gold standard" and CCTA may not provide a definite diagnosis of obstructive CAD in some cases. Lastly, a limited number of healthy individuals and patients were enrolled in this study, which sufficed for demonstrating the technical feasibility. While we did not conduct studies on vessel wall and plaque characterization, we anticipate that future technical advancements in MRI will facilitate the analysis of vessel wall and plaque.

In conclusion, the potential of 3D whole-heart non-contrast-enhanced DL-CS mDIXON coronary MRA has been confirmed in both healthy subjects and individuals with suspected CAD. The proposed DL-CS method notably enhanced image quality with a clinically acceptable scan duration and demonstrated excellent diagnostic performance when compared to CCTA as the reference
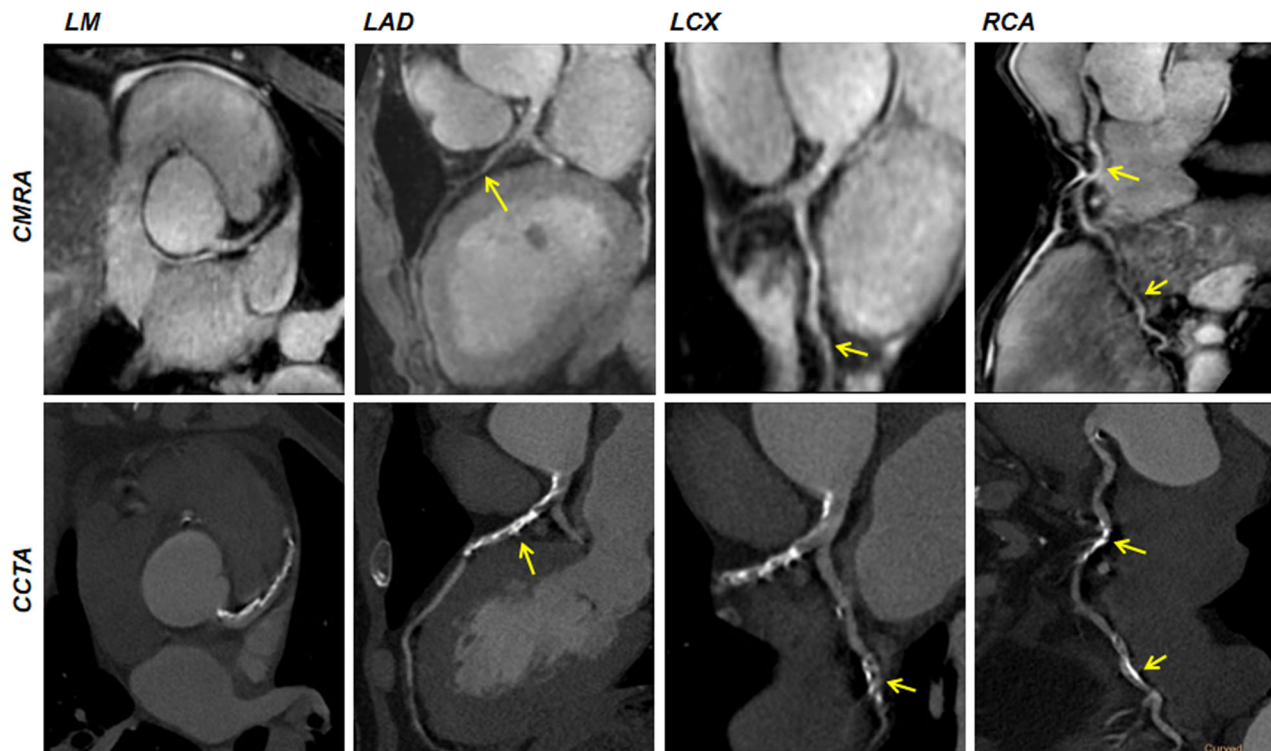
Wu *et al. Insights into Imaging* (2024)15:224

Page 10 of 12

Fig. 6 Curved planar reformation coronary MRA and CCTA images from a 63-year-old male patient with diffuse calcification and significant stenosis (≥ 50% diameter stenosis) (yellow arrows). Coronary MRA images show stenosis matching the lesion detected by CCTA. CCTA, coronary computed tomography angiography; CMRA, coronary magnetic resonance angiography; LAD, left anterior descending artery; LCX, left circumflex; LM, left main artery; RCA, right coronary artery

standard, which could be a viable alternative to enhance the clinical workflow of coronary MRA.

Abbreviations
bSSFP	Balanced steady-state free precession
CAD	Coronary artery disease
CCTA	Coronary computed tomography angiography
CS	Compressed sensing
DL	Deep learning
LAD	Left anterior descending
LCX	Left circumfex
mDIXON	Modified DIXON
MRA	Magnetic resonance angiography
RCA	Right coronary artery
SENSE	Sensitivity encoding

Supplementary information
The online version contains supplementary material available at https://doi.org/10.1186/s13244-024-01797-3.

┌───┐
│ Electronic supplementary material   │
└───┘

Authors contributions
X.W.: data collection, analysis, and writing. X.Y., P.P., L.L., S.H., and L.C.: data collection and analysis. X.T. and X.Z.: methodology. F.H., P.L., and J.S.: conception and supervision. All authors read and approved the final manuscript.

Data availability
The data used during the current study are available from the corresponding author upon reasonable request.

Declarations

Ethics approval and consent to participate
This study was approved by the Local Ethics Committee in accordance with the Declaration of Helsinki, as revised in 2013 (IRB no. 2016 355) and all participants gave written consent. The abstract of this manuscript has been accepted by ECR 2023.

Consent for publication
Not applicable.

Competing interests
The authors declare no competing interests.

Author details
[1]Department of Radiology, Hunan Provincial People's Hospital, The First Affiliated Hospital of Hunan Normal University, Changsha, China. [2]Department of Radiology, West China Hospital of Sichuan University, Chengdu, China. [3]Clinical Science, Philips Healthcare, Chengdu, China.

Wu *et al. Insights into Imaging* (2024)15:224

Page 11 of 12

References

1. Nagata M, Kato S, Kitagawa K et al (2011) Diagnostic accuracy of 1.5-T unenhanced whole-heart coronary MR angiography performed with 32-channel cardiac coils: initial single-center experience. Radiology 259:384–392
2. Yonezawa M, Nagata M, Kitagawa K et al (2014) Quantitative analysis of 1.5-T whole-heart coronary MR angiograms obtained with 32-channel cardiac coils: a comparison with conventional quantitative coronary angiography. Radiology 271:356–364
3. Kato Y, Ambale-Venkatesh B, Kassai Y et al (2020) Non-contrast coronary magnetic resonance angiography: current frontiers and future horizons. MAGMA 33:591–612
4. Zahergivar A, Kocher M, Waltz J et al (2021) The diagnostic value of non-contrast magnetic resonance coronary angiography in the assessment of coronary artery disease: a systematic review and meta-analysis. Heliyon 7:e06386
5. Gweon HM, Kim SJ, Lee SM et al (2011) 3D whole-heart coronary MR angiography at 1.5 T in healthy volunteers: comparison between unenhanced SSFP and Gd-enhanced FLASH sequences. Korean J Radiol 12:679–685
6. Zhao SH, Li CG, Chen YY et al (2020) Applying nitroglycerin at coronary MR angiography at 1.5 T: diagnostic performance of coronary vasodilation in patients with coronary artery disease. Radiol Cardiothorac Imaging 2:e190018
7. Correia T, Ginami G, Cruz G et al (2018) Optimized respiratory-resolved motion-compensated 3D Cartesian coronary MR angiography. Magn Reson Med 80:2618–2629
8. Kato S, Kitagawa K, Ishida N et al (2010) Assessment of coronary artery disease using magnetic resonance coronary angiography: a national multicenter trial. J Am Coll Cardiol 56:983–991
9. Kourtidou S, Jones MR, Moore RA et al (2019) mDixon ECG-gated 3-dimensional cardiovascular magnetic resonance angiography in patients with congenital cardiovascular disease. J Cardiovasc Magn Reson 21:52
10. Nezafat M, Henningsson M, Ripley DP et al (2016) Coronary MR angiography at 3T: fat suppression versus water–fat separation. MAGMA 29:733–738
11. Lu H, Zhao S, Tian D et al (2022) Clinical application of non-contrast-enhanced dixon water-fat separation compressed SENSE whole-heart coronary MR angiography at 3.0 T with and without nitroglyceri. J Magn Reson Imaging 55:579–591
12. Lu H, Guo J, Zhao S et al (2022) Assessment of non-contrast-enhanced dixon water–fat separation compressed sensing whole-heart coronary MR angiography at 3.0 T: a single-center experience. Acad Radiol 29:S82–S90
13. Dey D, Nakazato R, Li D et al (2012) Epicardial and thoracic fat-noninvasive measurement and clinical implications. Cardiovasc Diagn Ther 2:85–93
14. Yong HS, Kim EJ, Seo HS et al (2010) Pericardial fat is more abundant in patients with coronary atherosclerosis and even in the non-obese patients: evaluation with cardiac CT angiography. Int J Cardiovasc Imaging 26:53–62
15. Goeller M, Achenbach S, Cadet S et al (2018) Pericoronary adipose tissue computed tomography attenuation and high-risk plaque characteristics in acute coronary syndrome compared with stable coronary artery disease. JAMA Cardiol 3:858–863
16. Foley JRJ, Fent GJ, Garg P et al (2019) Feasibility study of a single breath-hold, 3D mDIXON pulse sequence for late gadolinium enhancement imaging of ischemic scar. J Magn Reson Imaging 49:1437–1445
17. Eggers H, Brendel B, Duijndam A et al (2011) Dual-echo Dixon imaging with flexible choice of echo times. Magn Reson Med 65:96–107
18. Akçakaya M, Basha TA, Chan RH et al (2014) Accelerated isotropic sub-millimeter whole-heart coronary MRI: compressed sensing versus parallel imaging. Magn Reson Med 71:815–822
19. Hajhosseiny R, Rashid I, Bustin A et al (2021) Clinical comparison of sub-mm high-resolution non-contrast coronary CMR angiography against coronary CT angiography in patients with low-intermediate risk of coronary artery disease: a single center trial. J Cardiovasc Magn Reson 23:57
20. Yokota Y, Takeda C, Kidoh M et al (2021) Effects of deep learning reconstruction technique in high-resolution non-contrast magnetic resonance coronary angiography at a 3-Tesla machine. Can Assoc Radiol J 72:120–127
21. Niendorf T, Hardy CJ, Giaquinto RO et al (2006) Toward single breath-hold whole-heart coverage coronary MRA using highly accelerated parallel imaging with a 32-channel MR system. Magn Reson Med 56:167–176
22. Gharib AM, Abd-Elmoniem KZ, Ho VB et al (2012) The feasibility of 350 mum spatial resolution coronary magnetic resonance angiography at 3 T in humans. Invest Radiol 47:339–345
23. Lin L, Wang L, Zhang X et al (2021) A clinical strategy to improve the diagnostic accuracy of 1.5-T non-contrast MR coronary angiography for detection of coronary artery disease: combination of whole-heart and volume-targeted imaging. Eur Radiol 31:1894–1904
24. Zhang Y, Zhang X, Jiang Y et al (2023) 3D whole-heart noncontrast coronary MR angiography based on compressed SENSE technology: a comparative study of conventional SENSE sequence and coronary computed tomography angiography. Insights Imaging 14:35
25. Deshmane A, Gulani V, Griswold MA et al (2012) Parallel MR imaging. J Magn Reson Imaging 36:55–72
26. Lustig M, Donoho D, Pauly JM (2007) Sparse MRI: the application of compressed sensing for rapid MR imaging. Magn Reson Med 58:1182–1195
27. Nakamura M, Kido T, Kido T et al (2018) Non-contrast compressed sensing whole-heart coronary magnetic resonance angiography at 3T: a comparison with conventional imaging. Eur J Radiol 104:43–48
28. Pezzotti N, Yousefi S, Elmahdy MS et al (2020) An adaptive intelligence algorithm for undersampled knee MRI reconstruction. IEEE Access 8:204825–204838
29. Qi H, Hajhosseiny R, Cruz G et al (2021) End-to-end deep learning non-rigid motion-corrected reconstruction for highly accelerated free-breathing coronary MRA. Magn Reson Med 86:1983–1996
30. Fuin N, Bustin A, Kustner T et al (2020) A multi-scale variational neural network for accelerating motion-compensated whole-heart 3D coronary MR angiography. Magn Reson Imaging 70:155–167
31. Hosseini S, Zhang C, Weingartner S et al (2020) Accelerated coronary MRI with sRAKI: a database-free self-consistent neural network k-space reconstruction for arbitrary undersampling. PLoS One 15:e0229418
32. Kobayashi H, Nakayama R, Hizukuri A et al (2020) Improving image resolution of whole-heart coronary MRA using convolutional neural network. J Digit Imaging 33:497–503
33. Ronneberger O, Fischer P, Brox T (2015) U-Net: convolutional networks for biomedical image segmentation. In: Navab N, Hornegger J, Wells WM, Frangi AF (eds) BT-medical image computing and computer-assisted intervention—MICCAI 2015. Springer International Publishing, Cham, pp 234–241
34. Foreman SC, Neumann J, Han J et al (2022) Deep learning-based acceleration of compressed sense MR imaging of the ankle. Eur Radiol 32:8376–8385
35. Wu X, Deng LP, Li WJ et al (2023) Deep learning-based acceleration of compressed sensing for non-contrast-enhanced coronary magnetic resonance angiography in patients with suspected coronary artery disease. J Magn Reson Imaging 58:1521–1530
36. Wu X, Tang L, Li WJ et al (2023) Feasibility of accelerated non-contrast-enhanced whole-heart bSSFP coronary MR angiography by deep learning-constrained compressed sensing. Eur Radiol 33:8180–8190
37. Cury RC, Leipsic J, Abbara S et al (2022) CAD-RADS™ 2.0—2022 coronary artery disease-reporting and data system: an expert consensus document of the society of cardiovascular computed tomography (SCCT), the American College of Cardiology (ACC), the American College of Radiology (ACR), and the North America Society of Cardiovascular Imaging (NASCI). JACC Cardiovasc Imaging 15:1974–2001
38. Li W, Diao K, Wen Y et al (2022) High-strength deep learning image reconstruction in coronary CT angiography at 70-kVp tube voltage significantly improves image quality and reduces both radiation and contrast doses. Eur Radiol 32:2912–2920
39. Börnert P, Koken P, Nehrke K et al (2014) Water/fat-resolved whole-heart Dixon coronary MRA: an initial comparison. Magn Reson Med 71:156–163
40. Mesropyan N, Isaak A, Dabir D et al (2021) Free-breathing high resolution modified Dixon steady-state angiography with compressed sensing for the assessment of the thoracic vasculature in pediatric patients with congenital heart disease. J Cardiovasc Magn Reson 23:117

Wu *et al. Insights into Imaging* (2024)15:224

Page 12 of 12

41. Munoz C, Cruz G, Neji R et al (2019) Motion corrected water/fat whole-heart coronary MR angiography with 100% respiratory efficiency. Magn Reson Med 82:732–742

42. Hirai K, Kido T, Kido T et al (2020) Feasibility of contrast-enhanced coronary artery magnetic resonance angiography using compressed sensing. J Cardiovasc Magn Reson 22:15

43. Kidoh M, Shinoda K, Kitajima M et al (2020) Deep learning based noise reduction for brain MR imaging: tests on phantoms and healthy volunteers. Magn Reson Med Sci 19:195–206

44. Wu Y, Tadamura E, Yamamuro M et al (2007) Evaluation of three-dimensional navigator-gated whole heart MR coronary angiography: the importance of systolic imaging in subjects with high heart rates. Eur J Radiol 61:91–96

Publisher's Note